

# Enhancement of Q-Switched Erbium-Doped Fibre Laser Performance using Graphene Oxide-Calcium Oxide Thin Film Saturable Absorbers

Muhammad Ilham Ahmad Zaini<sup>a</sup>, Abdul Rahman Johari<sup>a</sup>, Ganesan Krishnan<sup>a,b</sup>, Ahmad Fakhurrazi Ahmad Noorden<sup>c</sup>, Suzairi Daud<sup>a,b\*</sup>

<sup>a</sup>Department of Physics, Faculty of Science, Universiti Teknologi Malaysia, 81310 UTM Johor Bahru, Johor, Malaysia; <sup>b</sup>Laser Center, Ibnu Sina Institute for Scientific & Industrial Research (ISI-SIR), Universiti Teknologi Malaysia, 81310 UTM Johor Bahru, Johor, Malaysia; <sup>c</sup>Centre for Advanced Optoelectronics Research (CAPTOR), Kuliyyah of Science, International Islamic University Malaysia, 25200 Kuantan, Pahang, Malaysia

**Abstract** This paper presents an experiment utilizing calcium oxide (CaO) from the cuttlefish bone combined with graphene oxide (GO) to create a graphene oxide-calcium oxide (GO-CaO) based saturable absorber (SA) for Q-switched erbium-doped fibre lasers. The experiment aims to investigate the impact of calcium oxide when added to graphene oxide to form the SA thin film. The laser performance of both types of SA was compared, considering their input pump power, repetition rate, pulse width, and output power. The results indicated that the graphene oxide – calcium oxide SA thin film provided the best output power and the lowest threshold input pump power at 10.76  $\mu$ W and 53.12 mW, respectively. In the characterization, UV-Vis spectroscopy was utilized to determine the number of discrete wavelengths in UV or visible light that the materials absorbed or transmitted. The UV-Vis results indicated that the graphene oxide thin film exhibited an absorbance value of 0.049 AU and a transmittance value of 89.25 % at a wavelength of 1565 nm. In comparison, the GO-CaO SA thin film displayed an absorbance value of 0.037 AU and a transmittance value of 91.89 % at the same wavelength. Raman spectroscopy was also conducted to provide details about the chemical structure and crystallinity of the thin film samples. The results showed high-intensity peaks for the GO thin film at wavenumbers of 1353.74  $\text{cm}^{-1}$  and 1609.85  $\text{cm}^{-1}$ , and for GO – CaO thin film at wavenumbers of 1358.56  $\text{cm}^{-1}$  and 1612.18  $\text{cm}^{-1}$ . Additionally, SEM was utilized to study the morphology of the thin film samples. Based on the characterization and laser performance results, it was concluded that the addition of calcium oxide to graphene oxide enhances the properties of the SA thin film, leading to improved laser performance due to its higher thermal conductivity.

\*For correspondence:  
suzairidaud@utm.my

Received: 19 Feb. 2024  
Accepted: 11 June 2024

©Copyright Ahmad Zaini.  
This article is distributed  
under the terms of the  
[Creative Commons  
Attribution License](#), which  
permits unrestricted use  
and redistribution provided  
that the original author and  
source are credited.

**Keywords:** Saturable absorber, GO, GO – CaO, thin films, Q-switched laser.

## Introduction

Q-switching is a widely used technique in fibre laser applications for generating ultra-short laser pulses with high peak power. Compared with the mode-locking technique, Q-switching is the simpler way to implement, as it does not require fine-tuning the laser system's dispersion and nonlinearities [1,2]. The gain medium and SA work together in a passive Q-switched Erbium-doped fibre laser. SA transmits high-intensity light after absorbing low-intensity light. [3], while the gain medium stores energy and emits photons when pumped.

Various materials have been explored as SA in laser, such as graphene oxide (GO) [4], carbon nanotubes [5], and cadmium sulfide [1]. Nevertheless, these materials possess certain constraints that hinder attaining high output power, primarily stemming from their restricted operational range of wavelengths. This limits their application to specific laser sources, reducing the Q-switched laser system's flexibility and diversity. Generally, these materials have long recovery durations, which can restrict the maximum pulse length and repetition rate that a Q-switched laser can produce [6]. Faster recovery durations are required for generating shorter pulses and obtaining greater repetition rates.

To overcome this, we have investigated a material called calcium oxide (CaO), derived from cuttlefish bone (CFB), to improve the laser output power's thermal conductivity [7]. CaO has broadband absorption properties, which can absorb light at a wide variety of wavelengths [8]. This makes it appropriate to be used in SA thin films functioned with a variety of laser sources. CaO is chemically stable and resistant to moisture and oxidation. This stability provides the SA thin film's endurance and reliability, making it suited for long-term applications.

Furthermore, CaO is also known as marine debris. Marine debris is a significant environmental problem, with millions of tons generated every day. Recycling marine waste, such as cuttlefish bone, as an SA can help to address this problem. Thus, using green materials for Q-switched Erbium-doped fibre lasers can contribute to a more sustainable world.

According to Liang and Cai [12], the bulk of peer-to-peer (P2P) loans are granted based on borrowers' credit rather than mortgages. Due to a rise in loan requests from society, the author employed a deep learning strategy in this research, including an artificial neural network (ANN), a recurrent neural network (RNN), a long short-term memory (LSTM) model, and a gated recurrent unit (GRU). These models were compared to the standard time series model, ARIMA. The results reveal that the LSTM and GRU models outperform the other models. Weytjens *et al.* [13] also suggested using a machine learning approach to forecast cash flow. LSTM is compared against the ARIMA model, Facebook's TM Prophet, and multi-layered perceptron (MLP) in this study. Weytjens *et al.* [13] also recommended utilising a machine learning technique in estimating cash flow. With the goal of saving money, this study compared LSTM to the ARIMA model, Facebook's TM Prophet, and multi-layered perceptron (MLP). As a result, according to this study, LSTM and MLP perform better in projecting cash flow for this sort of data.

## Methodology

### Materials

ARIMA GO and GO-CaO thin film were utilized to measure the performance of the laser system and the properties of the SA thin film. GO's functional groups, including hydroxyl and epoxide groups, allow it to disperse in water [9]. This enables GO to be mixed easily with PVA into a well-mixed solution, as PVA will help to glue the molecules inside the solution.

Figure 1 shows the fundamental structure of graphene and GO, where GO's functional groups can be observed. Additionally, compared to graphene, GO has a high density of oxygen functional groups, which aids in the dissolution of water and organic solvents [10]. The produced GO has a high hydroxyl content, facilitating the fabrication of films on the substrate for Q-switching element production. Consequently, the properties of GO make it a more straightforward choice for manufacturing SA than graphene.

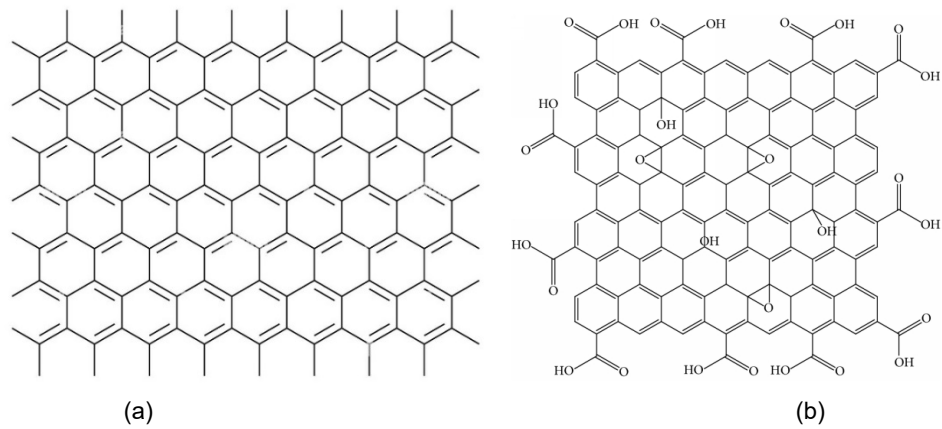


**Figure 1.** A fundamental structure of (a) graphene and (b) graphene oxide

The experiment involved the selection of new material, specifically cuttlefish bone, as shown in Figure 2. The cuttlefish bone (CFB) sample was collected from Teluk Ketapang Beach in Terengganu, where it can be conveniently sourced. The main component of CFB is primarily calcium oxide (CaO). CFB shell matrix and the dorsal shield make up the CFB. The internal shell of the bone is brittle and laminar, serving as a buoyancy tank for cuttlefish, while the robust and dense dorsal shield of the bone provides a firm substrate. Calcium carbonate makes up the majority of CFB, from which CaO can be produced.



**Figure 2.** The architectural of multilayer perceptron neural network

The precipitation method was employed for the production of CaO. In this method, cuttlefish bones were cleaned in distilled water, air-dried, and powdered. The CFB were then heated at room temperature at a rate of 5 °C/min until reaching 1300 °C. The samples were annealed for four hours at temperatures ranging from 200 to 1200 °C, with each temperature increment of 100 °C, to obtain the CaO [11].

### Preparation of Graphene Oxide Saturable Absorber Thin Film Model

10 mL of PVA solution and five mL of GO solution were mixed and agitated for two hours with a magnetic stirrer [13]. The GO oxide and PVA solution were subjected to ultra-sonication for a duration of 30 to 60 minutes to ensure the complete dissolution and uniform dispersion of all the GO nanoparticles to produce GO solution for the SA thin film.

## Preparation of Graphene Oxide-Calcium Oxide Saturable Absorber Thin Films

To prepare the SA thin film to be used in an Erbium-doped fibre laser, cuttlefish bone was crushed using an agate mortar and then subjected to a calcination process inside a furnace at 700 °C for five hours to produce CaO in powder form [12].

The CaO nanoparticles were then incorporated into a polyvinyl alcohol (PVA) matrix, starting with the mixing of one gram of PVA powder with 80 mL of deionized water, and agitated for one hour using a magnetic stirrer. The mixture was then placed in an ultrasonic bath for one hour to ensure thorough blending. It was then followed by adding 20 mL of GO solution to the mixture, which was agitated for a further two hours at room temperature using a magnetic stirrer.

Subsequently, 10 mL of PVA solution was added to the 20 mL GO-CaO mixture and agitated for an hour. The mixture was then placed in an ultrasonic bath for 30 minutes to ensure the complete dissolution of the GO nanoparticles. The resulting liquid was deposited in a small petri dish and allowed to dry for 72 hours using the drop-cast technique to form a composite SA thin film, as shown in Figure 3(a).

This process produced a new SA thin film, with the addition of CaO nanoparticles to the GO, which served as the second sample for this research. The first sample is composed solely of GO, as shown in Figure 3(b). Both samples were then used as SA thin films in the passive Q-switched Erbium-doped fibre lasers.

## Preparation of Graphene Oxide Saturable Absorber Thin Film Model

In this study, the hybrid model will be a mix of Holt-Winter's and single exponential smoothing (SES). The Holt-Winter's technique will be used in this study since the data shows a trend and seasonal pattern and in the second process of the hybrid model, the SES model was chosen to execute the hybrid model because the error yields from the forecast of the Holt-Winter's will usually generate a stationary pattern of residual. There will be three smoothing constants used:  $\alpha$ ,  $\beta$ , and  $\gamma$ . The general formula for the Holt-Winter's model is given as follows:



(a)



(b)

**Figure 3.** (a): Drop-cast solution and (b): Dried solution of SA thin film

## Experimental Setup for the Measurement of Q-switched Erbium-doped Laser System's Performance

The Erbium-doped fibre laser setup is shown in Figure 4. A ring cavity is present in the laser, which helps make the laser operate continuously and emits a short and stable pulse through a passive Q-switched technique. A 45 cm piece of Erbium-doped fibre will be employed as a gain medium. The single-mode fibre (SMF) comprised the rest of the cavity, which had a total length of 42 meters.

A wavelength division multiplexer pulsed the laser with a 980 nm laser diode was also utilized. The GO and GO-CaO SA thin film, made using the chemical vapor deposition (CVD) process, served as a passive Q-switcher. To change the polarization state of the circulating light and optimize the Q-switching operation, a polarization controller (PC) was used. The laser's unidirectional operation was ensured via an optical isolator.

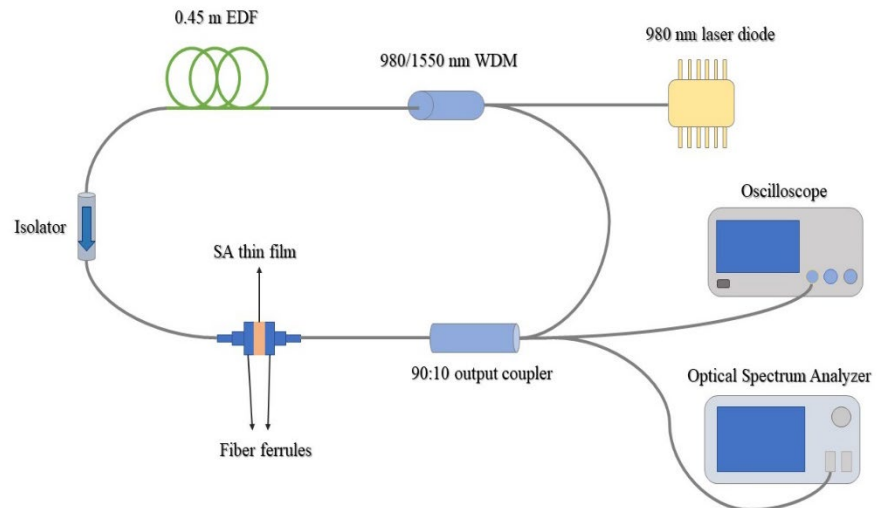


**Figure 4.** Experimental setup of passive Q-switched Erbium-doped fibre laser

## Characterization Measurement by UV-Vis, Raman Spectroscopy and SEM

The samples were characterised using a combination of UV-Vis spectroscopy, Raman spectroscopy, and scanning electron microscopy (SEM). The amount of light absorbed by the chemical components in the samples was calculated using UV-Vis spectroscopy. This was achieved by measuring the intensity of light entering the sample and comparing it to a reference PVA thin film over a 200–2000 nm wavelength range. To measure the absorbance of the SA substance, UV-Vis spectroscopy was set to focus on a wavelength range of 200 nm to 2000 nm.

Raman spectroscopy was utilized to detect the vibrational, rotational, and other states in the molecular system, allowing for the identification of the chemical composition of materials such as GO and GO-CaO SA thin films. SEM was utilized to directly examine the surfaces of solid objects, including thin films, owing to its high resolution

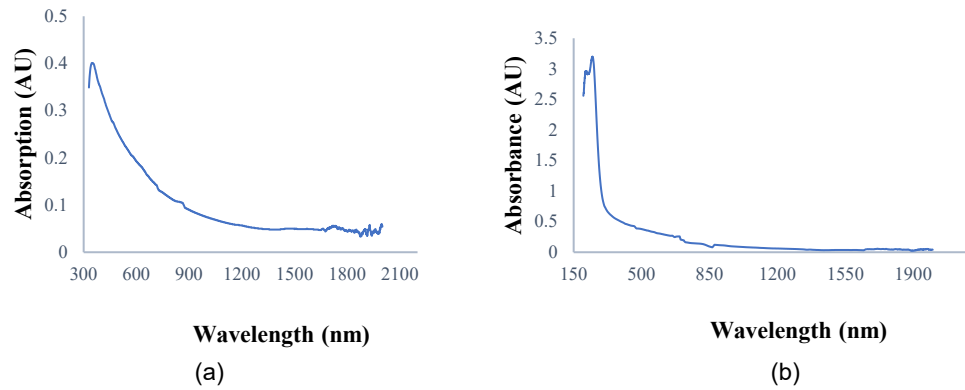
## Preparation of Graphene Oxide Saturable Absorber Thin Film Model

In this study, the hybrid model will be a mix of Holt-Winter's and single exponential smoothing (SES). The Holt-Winter's technique will be used in this study since the data shows a trend and seasonal pattern and in the second process of the hybrid model, the SES model was chosen to execute the hybrid model because the error yields from the forecast of the Holt-Winter's will usually generate a stationary pattern of residual. There will be three smoothing constants used:  $\alpha$ ,  $\beta$ , and  $\gamma$ . The general formula for the Holt-Winter's model is given as follows:

## Result and Discussion

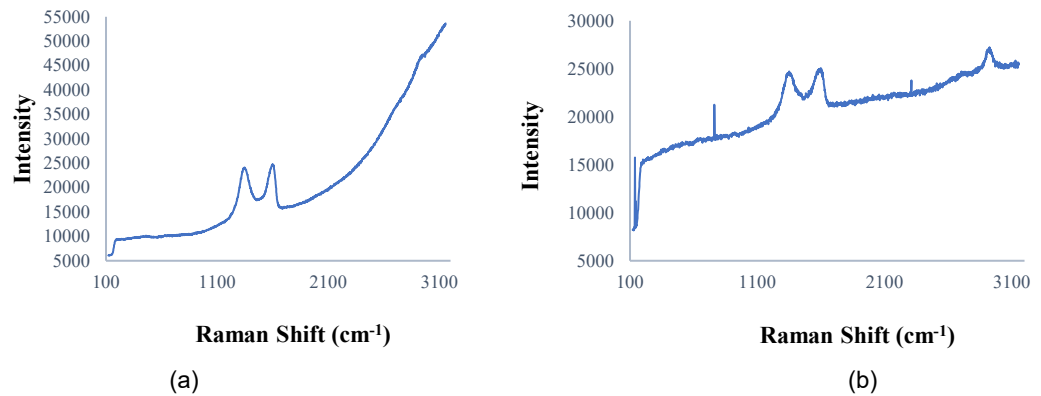
### Characterization of the SA Material Thin Film by UV-Vis, Raman Spectroscopy and Scanning Electron Microscope

Figure 5 illustrates the absorbance spectra obtained from UV-Vis spectroscopy characterization for both GO and GO-CaO samples. The graph plotted shows that the absorbance value for GO is 0.049 AU, while the GO-CaO exhibits an absorbance value of 0.037 AU.



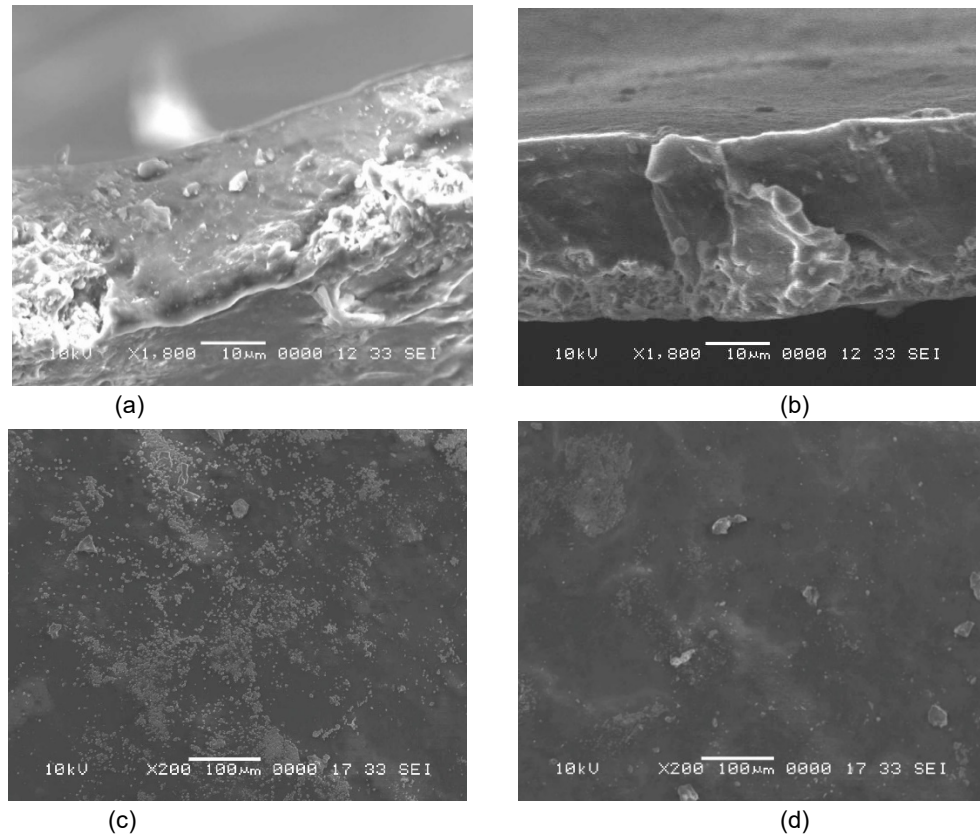
**Figure 5.** UV-Vis Spectroscopy (a) GO. (b) GO-CaO

Figure 6 displays the Raman spectra with high-intensity peaks observed at wavenumbers of 1353.74  $\text{cm}^{-1}$  and 1609.85  $\text{cm}^{-1}$  for the GO thin film and at wavenumbers of 1358.56  $\text{cm}^{-1}$  and 1612.18  $\text{cm}^{-1}$  for the GO-CaO thin film. These high-intensity peaks exhibit only slight shifts in value. Previous research has shown that Raman spectroscopy for GO is characterized by a G band at 1605  $\text{cm}^{-1}$ , which relates to the E2 phonon of the  $\text{sp}^2$  C atoms, and a D band at 1353  $\text{cm}^{-1}$ , corresponding to the breathing mode of  $\kappa$  point phonons of A1g symmetry, indicating disorder caused by defects such as vacancies, grain boundaries, and amorphous carbon species [14,15]. The surface morphology of the GO and GO-CaO SA thin film was examined using a scanning electron microscope (SEM, JSM-5510LV, JEOL), and the films' quality was evaluated.



**Figure 6.** Raman Spectroscopy (a) GO. (b) GO-CaO

Figures 7 (a) and (b) show the side-view images of the thin film with a magnification of 1800x, while Figures 7 (c) and (d) display the top surface of the thin film at a smaller magnification of 200x. The SEM image revealed that the surface of the thin film was nearly even, mixed between the GO, CaO, and PVA.



**Figure 7.** SEM image for the 2 SA thin films. Side view (a) GO, (b) GO-CaO; Top view (c) GO, (d) GO-CaO

### Laser System's Performance for Different SAs

This section compares the laser performance of GO SA and GO-CaO SA thin films in terms of repetition rate, pulse width, and output power. This measurement was done using an oscilloscope and OSA. Voltage signals were examined on the oscilloscope and shown as waveforms, which are graphic depictions of voltage variation over time. A graph was used to display the signals and show how they changed over time. The horizontal (X) axis represents time, while the vertical (Y) axis represents voltage measurement.

On the other hand, the main focus of OSA was the detection of small changes in the position of the wave signal when the SA thin film was sandwiched between two fibre ferrules. This change was compared to the free running value (without SA) to observe whether the laser optical signal shifted to the left or right side. Changes in the pulse repetition rate can be deduced by analyzing the shift in the laser output. A shift to the left could imply an increase in the pulse repetition rate, whilst a change to the right could indicate a decrease. This data is useful for optimizing laser performance and fine-tuning the laser for specific applications.

Figures 8(a) and 8(b) depict the pulse repetition rate and pulse widths as a function of the pump power from the laser diode for GO and GO-CaO, respectively. The graph illustrates that the repetition rate increases as the pump power is raised. This occurs because an increase in pump power causes an increase in the power of the laser signal, which moves the graphene oxide-based SA towards the saturation phase [16]. The saturation level of the SA determines the production of laser pulses. Additionally, the pulse width of the generated laser pulses decreases as the pump power increases. This finding is consistent with typical Q-switched pulse behavior, where repetition rate and pulse width vary with pump power, as reported in references such as Nd: YAG laser passively Q-switched by graphene-oxide SA [17].

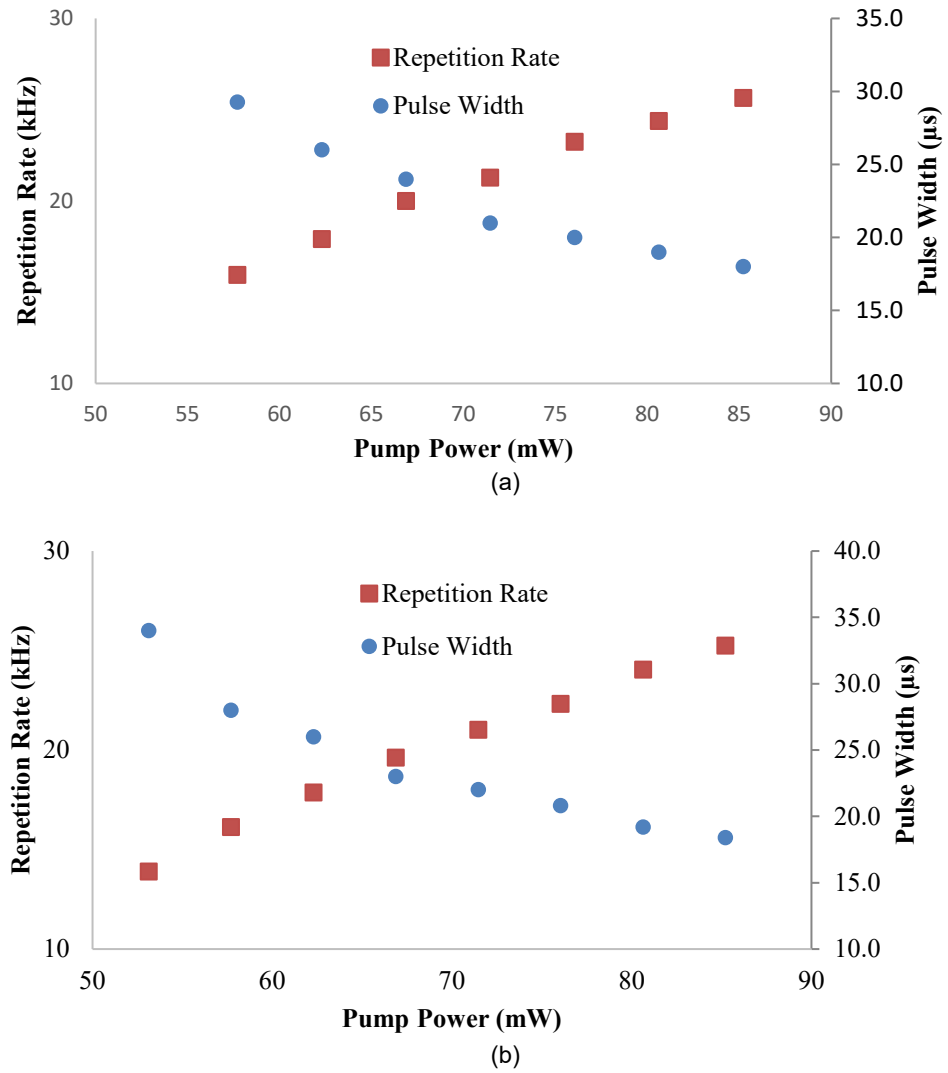
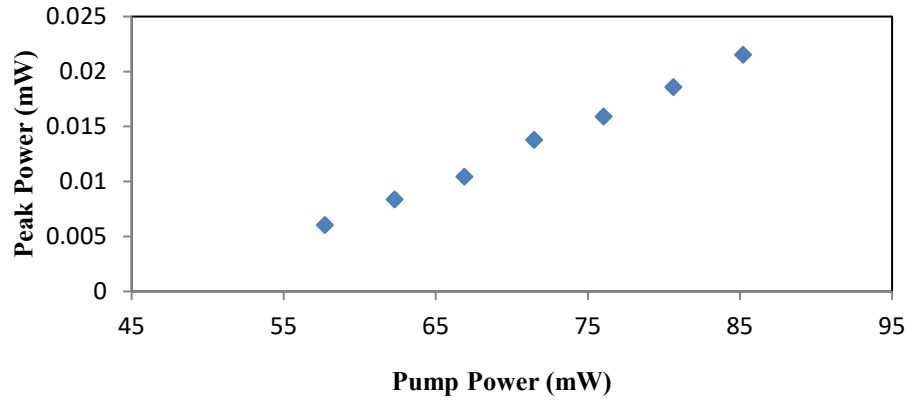


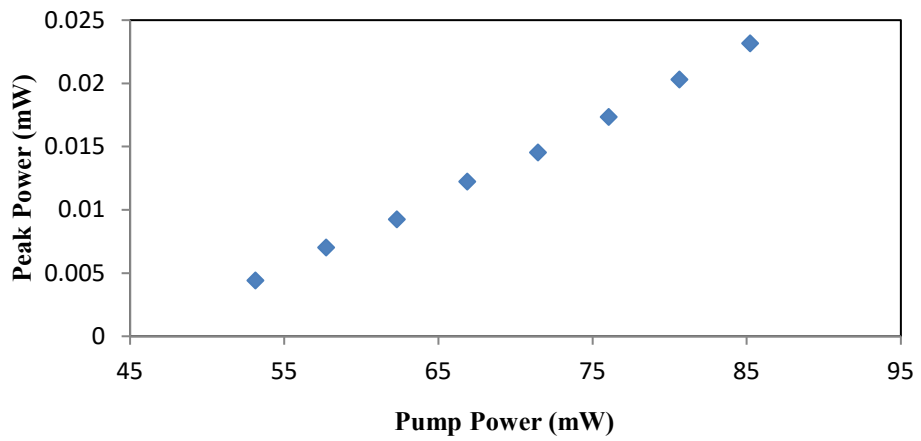
**Figure 8.** Graph of the repetition rate and pulse width with different pump powers for (a) GO; (b) GO-CaO

Figures 9 (a) and (b) illustrate the impact of pump power on peak power for both GO and GO-CaO thin films. The peak power of the laser signal for GO thin film increases from approximately 6.05 to 21.54  $\mu\text{W}$ , whereas for GO-CaO thin film, it increases from around 4.41 to 23.16  $\mu\text{W}$ . These findings demonstrate that as the input pump power rises from its lowest to the highest value, the laser performance's peak power also increases.





(a)



(b)

**Figure 9.** Graph of the peak power of the laser at different pump powers: (a) GO, (b) GO-CaO

### Comparison of the Laser System’s Performance of Different Sas

In To prepare the SA thin film to be used in an Erbium-doped fibre laser, cuttlefish bone was crushed using an agate mortar and then subjected to a calcination process inside a furnace at 700 °C for five hours to produce CaO in powder form [12].

**Table 1.** Comparison of the laser system’s performance by GO-CaO and GO SA thin film at the same input pump power.

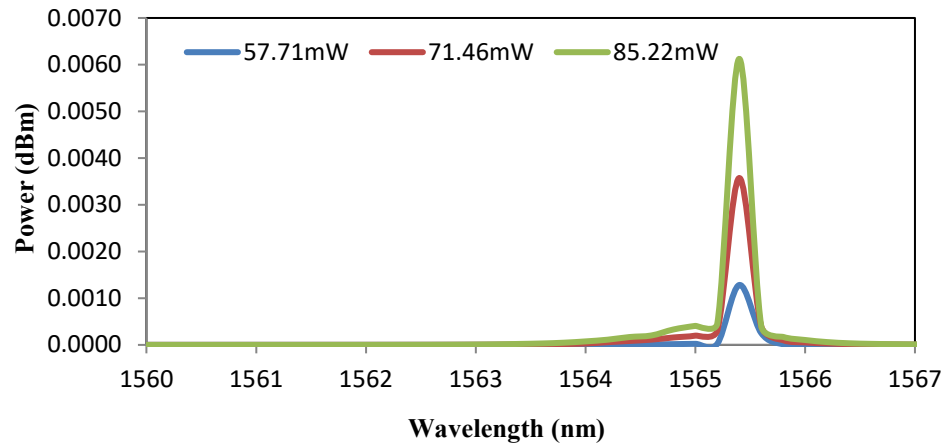
	GO	GO-CaO
<b>Lowest Input Power (mW)</b>	57.71	53.12
<b>Repetition Rate (kHz)</b>	25.64	25.25
<b>Pulse Width (µs)</b>	18.0	18.4
<b>Highest Output Power (µW)</b>	9.94	10.76

### Stability Performance of The Laser System

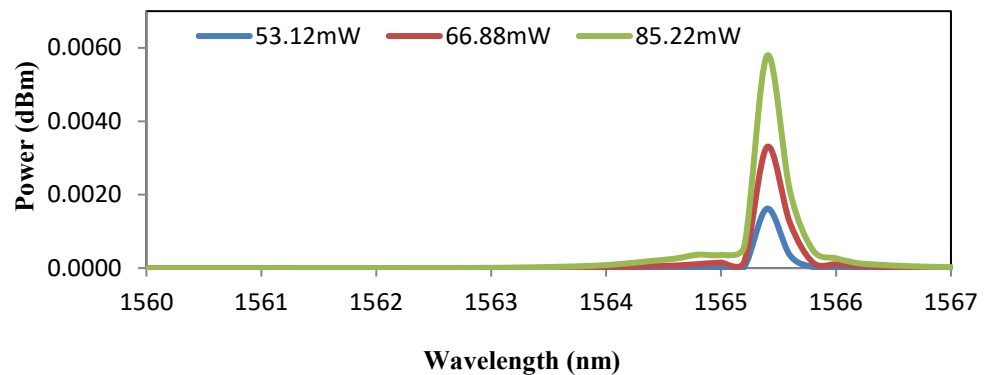
The OSA was utilized to evaluate the stability performance of the Q-switched Erbium-doped fibre laser with GO and GO-CaO thin films as the SA. SA devices have drawn the interest of researchers seeking to generate pulsed lasing in recent years due to their ease of usage and inexpensive fabrication cost

[20]. The OSA measures and displays the power distribution of an optical source over a specific wavelength range. Figure 10 (a) shows a comparison of the OSA for three different input pump powers for the GO SA thin film. This comparison aims to determine the stability of the generated laser pulses. The results show that the highest power (intensity) from the three different input pump powers was produced at the same wavelength of around 1565.4 nm, indicating that the laser-generated with GO as the SA thin film is stable across the various pump powers used.

Similarly, the OSA was used to compare the stability of the laser-generated with GO-CaO SA thin film for three different input pump powers. The results shown in Figure 10 (b) demonstrate that the highest power (intensity) from the three distinct input pump powers were produced at the same wavelength of approximately 1565.4 nm. This indicates that the laser generated for the Q-switched Erbium-doped fibre laser using GO-CaO as the SA thin film is also a stable pulse laser.



(a)



(b)

**Figure 10.** OSA comparison for 3 different input powers for Q-switched laser by (a) GO; (b) GO-CaO

## Conclusions

In conclusion, the GO-CaO compound is superior to GO as SA thin film in a Q-switched Erbium-doped fibre laser. The laser system's performance in terms of input pump power and output power shows that GO-CaO requires lower power to produce a Q-switched laser and produces higher output power values, which are 53.12 mW and 10.76  $\mu$ W respectively, while GO produces 57.71 mW and 9.94  $\mu$ W, respectively. The addition of CaO in the thin film improves the thin film's thermal conductivity, thus improving the output power of the laser. The UV-Vis spectroscopy analysis of the GO-CaO thin film shows an absorbance and transmittance value of 0.037 AU and 91.89 %, respectively, at a wavelength of 1565 nm. The Raman spectroscopy analysis shows high-intensity peaks at the wavenumbers' value of 1358.56  $\text{cm}^{-1}$  and 1612.18  $\text{cm}^{-1}$  for the GO-CaO thin film, indicating its potential to produce a better

SA material. The study shows that the laser beam created throughout the experiment was a stable pulse laser, as indicated by the OSA results.

## Conflicts of Interest

The author(s) declare(s) that there is no conflict of interest regarding the publication of this paper.

## Acknowledgement

This work was supported by Universiti Teknologi Malaysia in term of facilities and financially by the UTM Encouragement Grant vot no. Q.J130000.3854.31J54.

## References

- [1] Radzi, N., Latif, A., Ismail, M., Liew, J., Wang, E., Lee, H., Tamcheck, N., Awang, N., Ahmad, F., Halimah, M., & Ahmad, H. (2020). Q-switched fibre laser based on CdS quantum dots as a saturable absorber. *Results in Physics*, *16*, 103123.
- [2] Chen, Y., Jiang, G., Chen, S., Guo, Z., Yu, X., Zhao, C., Zhang, H., Bao, Q., Wen, S., Tang, D., & Fan, D. (2015). Mechanically exfoliated black phosphorus as a new saturable absorber for both Q-switching and mode-locking laser operation. *Optics Express*, *23*(10), 12823.
- [3] Ismail, M. A., Harun, S. W., Ahmad, H., & Paul, M. C. (2016). Passive Q-switched and mode-locked fibre lasers using carbon-based saturable absorbers. *Fibre Laser*.
- [4] Chang, J., Li, H., Yang, Z., & Yan, N. (2018). Efficient and compact Q-switched green laser using graphene oxide as saturable absorber. *Optics & Laser Technology*, *98*, 134–138.
- [5] Huda, C., Yasin, M., Harun, S., Jafry, A. A. A., & Rosol, A. H. A. (2020). Q-switched erbium-doped fibre laser incorporating multi-walled carbon nanotubes as a saturable absorber. *IOP Conference Series: Materials Science and Engineering*, *854*(1), 012059.
- [6] Ahmed, M. H. M., Ali, N. M., Salleh, Z. S., Rahman, A. A., Harun, S. W., Manaf, M., & Arof, H. (2015). Q-switched erbium-doped fibre laser based on single and multiple walled carbon nanotubes embedded in polyethylene oxide film as saturable absorber. *Optics & Laser Technology*, *65*, 25–28.
- [7] Nguyen, D. K., On, V. V., Hoat, D. M., Rivas-Silva, J. F., & Coccoletzi, G. H. (2021). Structural, electronic, magnetic and optical properties of CaO induced by oxygen incorporation effects: A first-principles study. *Physics Letters A*, *397*, 127241.
- [8] Liu, Z., Zhang, X., Yan, X., Chen, Y., & Tian, J. (2012). Nonlinear optical properties of graphene-based materials. *Chinese Science Bulletin*, *57*(23), 2971–2982.
- [9] Darwish, A. S., Sayed, M. A., & Shebl, A. (2020). Cuttlefish bone stabilized Ag<sub>3</sub>VO<sub>4</sub> nanocomposite and its Y<sub>2</sub>O<sub>3</sub>-decorated form: Waste-to-value development of efficiently eco-friendly visible-light-photoactive and biocidal agents for dyeing, bacterial and larvae depollution of Egypt's wastewater. *Journal of Photochemistry and Photobiology A: Chemistry*, *401*, 112749.
- [10] Neklyudov, V. V., Khafizov, N. R., Sedov, I. A., & Dimiev, A. M. (2017). New insights into the solubility of graphene oxide in water and alcohols. *Physical Chemistry Chemical Physics*, *19*(26), 17000–17008.
- [11] Faksawat, K., Sujinnapram, S., Limsuwan, P., Hoonvathana, E., & Naemchanthara, K. (2015). Preparation and characteristic of hydroxyapatite synthesized from cuttlefish bone by precipitation method. *Advanced Materials Research*, *1125*, 421–425.
- [12] Hassan, M. A. M., Mohammed, A. H., & Mahdi, W. B. (2021). Synthesis of hydroxyapatite nanostructures using chemical method. *Nano Biomedicine and Engineering*, *13*(3).
- [13] Qi, X., Yao, X., Deng, S., Zhou, T., & Fu, Q. (2014). Water-induced shape memory effect of graphene oxide reinforced polyvinyl alcohol nanocomposites. *Journal of Materials Chemistry A*, *2*(7), 2240–2249.
- [14] Johra, F. T., Lee, J.-W., & Jung, W.-G. (2014). Facile and safe graphene preparation on solution-based platform. *Journal of Industrial and Engineering Chemistry*, *20*(5), 2883–2887.
- [15] Behunová, M., Gallios, G., Girman, V., Kolev, H., Kaňuchová, M., Dolinská, S., & Václavíková, M. (2021). Electrophoretic deposition of graphene oxide on stainless steel substrate. *Nanomaterials*, *11*(7), 1779.
- [16] Ahmad, H., Zulkifli, A. Z., Kiat, Y. Y., & Harun, S. W. (2014). Q-switched fibre laser using 21 cm bismuth-erbium doped fibre and graphene oxide as saturable absorber. *Optics Communications*, *310*, 53–57.
- [17] Lin, H. Y., & Zhang, J. Y. (2018). Nd: YAG laser at 1112.3 nm passively Q-switched by graphene-oxide saturable absorber. *Optik*, *156*, 265–267.
- [18] Selivanov, E. N., Gulyaeva, R. I., Zaripov, R. Z., Sel'menskikh, N. I., & Marshuk, L. A. (2020). Effect of calcium oxide on the structure and the thermal properties of granulated high-iron slags. *Russian Metallurgy (Metally)*, *2020*(2), 121–126.
- [19] Baranda, P. S., Knudsen, A. K., & Ruh, E. (1993). Effect of CaO on the thermal conductivity of aluminium nitride. *Journal of the American Ceramic Society*, *76*(7), 1751–1760.
- [20] Jiang, T., Yin, K., Wang, C., You, J., Ouyang, H., Miao, R., Zhang, C.-X., Wei, K., Li, H., Chen, H., Zhang, R., Zheng, X., Xu, Z., Cheng, X., & Zhang, H. (2019). Ultrafast fibre lasers mode-locked by two-dimensional materials: Review and prospect. *Journal of Laser Micro Nanoengineering*, *8*(1), 78–78.